

Smith Chart Approach to the Design of Multilayer Resistive Sheet

C. P. Neo, Y. J. Zhang, W. J. Koh, L. F. Chen, C. K. Ong, and J. Ding

Abstract—The design of the multilayer resistive sheet is often given in some formulae or in some tabulated forms. The electrical engineer or material scientist often cannot visualize how the design really works or the achievable bandwidth. In this paper, we attempt to give a good understanding of the design of the multilayer resistive sheet by using the Smith Chart Approach. The Smith Chart Approach offers more flexibility to the design of the multilayer resistive sheet, as compared to published formulae or tables.

Index Terms—Bandwidth, design, multilayer resistive sheet, Smith Chart, visualization.

I. INTRODUCTION

THE Salisbury screen has been examined by a number of authors [1]–[3] some years ago, and has been widely used in practice. The multilayer resistive sheet, as shown in Fig. 1, consists of resistive sheets separated by lossless dielectric spacers of dielectric constant of 1 (denoted by ϵ_0 and μ_0). Although, it is impossible to have lossless dielectric spacers of dielectric constant of one in practice, nevertheless, the Smith Chart Approach is still applicable to other dielectric spacers. The purpose of adding layers is to increase the bandwidth. As shown in [4]–[7], the bandwidth is dependent not only on the number of layers, but also on the resistivity of the sheets. Hence, a three-layer resistive sheet with optimum resistive sheet values can have a wider bandwidth than a seven-layer resistive sheet with nonoptimum values.

Generally, it is essential to design the multilayer resistive sheet using the minimum number of resistive layers to achieve the maximum bandwidth for a given acceptable level of reflectivity. Although, there are a number of available design data for the multilayer resistive sheet [4]–[7], we attempt to give a good understanding of the design of the multilayer resistive sheet by using the Smith Chart Approach.

II. TRANSMISSION LINE THEORY

Fig. 1 shows the multilayer resistive sheet placed in front of a short circuit (metal backing). The loss is incorporated in the resistive sheets which are spaced a quarter wavelength apart.

Manuscript received May 14, 2002; revised July 23, 2002. The review of this letter was arranged by Associate Editor Dr. Shigeo Kawasaki.

C. P. Neo, Y. J. Zhang, and W. J. Koh are with the DSO National Laboratories, Singapore 118230 (e-mail: nchyepoh@dsi.org.sg).

L. F. Chen is with the Temasek Laboratories, National University of Singapore, Singapore 119260 (e-mail: tsclcf@nus.edu.sg).

C. K. Ong is with the Physics Department, National University of Singapore, Singapore 119260 (e-mail: phyongck@nus.edu.sg).

J. Ding is with the Materials Science Department, National University of Singapore, Singapore 119260 (e-mail: masdingj@nus.edu.sg).

Digital Object Identifier 10.1109/LMWC.2002.807710

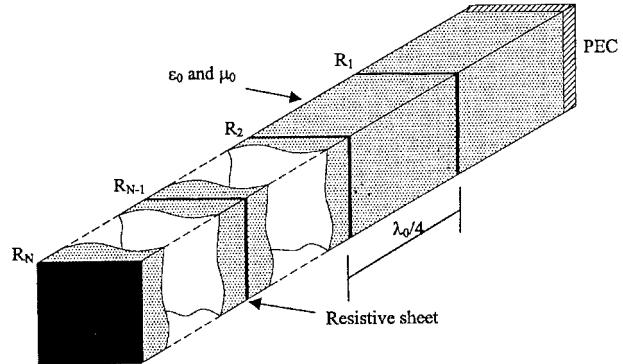


Fig. 1. Multilayer resistive sheet.

The resistive sheets attempt to match the free space impedance to the short circuit.

Using transmission line theory, the complex reflection coefficient at normal incidence of the lossy transmission structure is obtained as

$$S_{11} = \frac{Y_0 - Y_N}{Y_0 + Y_N} \quad (1)$$

$$Y_i = B_i + Y_0 \frac{Y_{i-1} + Y_0 \tanh(\vartheta)}{Y_0 + Y_{i-1} \tanh(\vartheta)}, i = 2, 3, \dots, N \quad (2)$$

$$Y_1 = B_1 + Y_0 \coth(\vartheta) \quad (3)$$

$$B_i = \frac{1}{R_i} \quad (4)$$

$$\vartheta = j \frac{\pi}{2} \frac{f}{f_0} \quad (5)$$

where Y_0 is the free-space admittance, R_i is the surface resistivity of the i^{th} layer, and f_0 is the center frequency.

In this paper, the relative bandwidth w is defined as

$$w = \frac{f_2 - f_1}{f_0} \quad (6)$$

where f_2 and f_1 are the -20 dB points for $|S_{11}|$.

III. DESIGN OF MULTILAYER RESISTIVE SHEET

Before we proceed with multilayer resistive sheet design, let us first understand the design of the Salisbury screen (single layer resistive sheet). In order to obtain zero reflectivity of the Salisbury screen at frequency f_0 , the short circuit impedance (marked \square in Fig. 2) is first transformed to the open circuit impedance (marked \times in Fig. 2) via a spacer of a quarter wavelength thick. The open circuit impedance is rotated 180° to obtain its equivalent admittance (marked \square in Fig. 2). Then, by adding a parallel resistive sheet with a resistivity that is equal

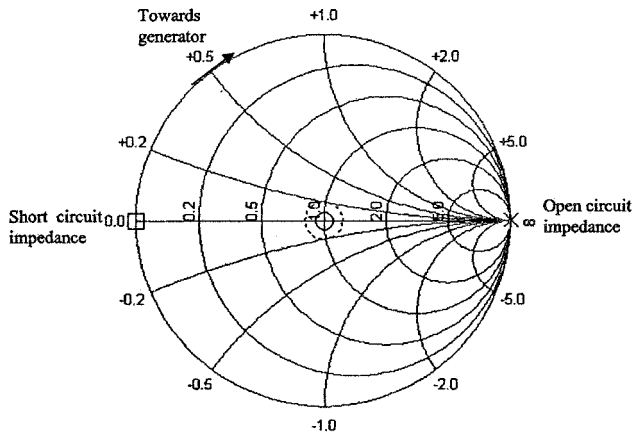


Fig. 2. Example to obtain zero reflectivity at frequency f_0 for one-layer resistive sheet.

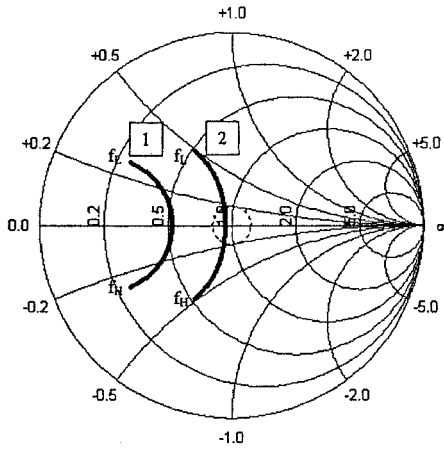


Fig. 3. $R_1 = 200 \Omega/\square$ and $R_2 = 700 \Omega/\square$ for a two-layer resistive sheet (1 denotes impedance curve for first layer and 2 denotes impedance curve for second layer).

to free-space impedance, the reflectivity of the screen becomes zero (marked O in Fig. 2).

The simulation results in this paper uses the step size of $1 \Omega/\square$ and $0.01 f_0$. The frequency range is $0.3 f_0(f_L)$ to $1.7 f_0(f_H)$. By using (1) and (3), the computed optimum bandwidth of the single-layer resistive sheet is 0.24 when the surface resistivity, R_1 , is any value between 347 and 395 Ω/\square .

Figs. 3 and 4 present the impedance curves of a two-layer resistive sheet with spacer thickness same as $\lambda_0/4$ and different R_1 . Their reflection coefficient curves can be obtained simply by taking the ratio of the length of the impedance points from the center of the Smith Chart to the radius of the Smith Chart. Fig. 3 illustrates the case of getting a single null in the reflection coefficient curve while Fig. 4 illustrates the case of getting two nulls in the reflection coefficient curve. It is noted that the value of R_1 has to be less than the free space impedance so that its impedance curve of the first layer resistive sheet is always on the left hand side of the -20 -dB circle (the -20 -dB circle is denoted by dotted line). Once B_1 is chosen, B_2 has to be a value for which B_2/Y_0 has to be smaller than $2(B_1/Y_0 - 1)$ but greater than $(B_1/Y_0 - 1)$ in order to move the impedance curve toward the -20 dB circle, see Figs. 3 and 4. Generally, in the design of N -layer resistive sheet, $R_1 < R_2 < R_3 \dots < R_{N-1} < R_N$ and $R_1 < 120\pi \Omega/\square$.

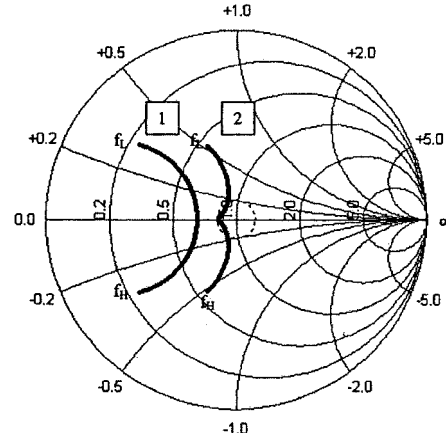


Fig. 4. $R_1 = 250 \Omega/\square$ and $R_2 = 700 \Omega/\square$ for a two-layer resistive sheet (1 denotes impedance curve for first layer and 2 denotes impedance curve for second layer).

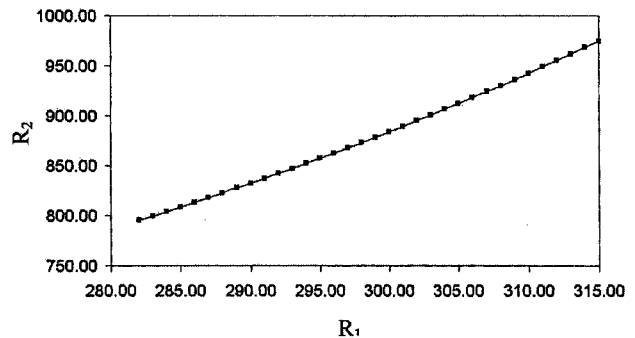


Fig. 5. Optimized R_1 and R_2 to obtain bandwidth of 0.86.

The design strategy for the two-layer resistive sheet is as follows.

a) For each B_1 , the value of B_2 is obtained for which the normalized admittance of two-layer resistive sheet equals to 1.222 at frequency f_0 .

b) With each pair of B_1 and B_2 , we compute f_2 .

f_2 is found to be $1.43 f_0$ and, therefore, $w = 0.86$, which agrees very well with [7]. Fig. 5 shows optimized pair of R_1 and R_2 to obtain bandwidth of 0.86. It is noted that the optimized pair of R_1 and R_2 give two nulls in the reflection coefficient curve of the two-layer resistive sheet.

Fig. 6 shows an example of obtaining three nulls on the reflection coefficient curve of a three-layer resistive sheet with spacer thickness same as $\lambda_0/4$. For the design of the three-layer resistive sheet, we have to find the optimum values of R_1 , R_2 , and R_3 to obtain two impedance points on the -20 dB curve (denoted by P and Q in Fig. 6). The design strategy for the three-layer resistive sheet is as follows.

a) The admittance before adding B_3 is given by

$$Y = Y_3 - B_3 = Y_0 \frac{Y_2 + Y_0 \tan h(\vartheta)}{Y_0 + Y_2 \tan h(\vartheta)}. \quad (7)$$

Adding B_3 only changes the conductance in Y . The conductance, g , on the -20 -dB circle for a given sucep-

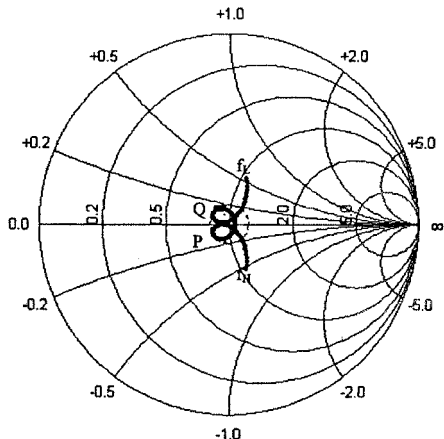


Fig. 6. $R_1 = 330 \Omega/\square$, $R_2 = 671 \Omega/\square$, and $R_3 = 1560 \Omega/\square$ for a three-layer resistive sheet.

stance, x , can be obtained solving the following quadratic equation:

$$(1 - r^2)g^2 - 2(1 + r^2)g + 1 - r^2 + x^2 - r^2x^2 = 0 \quad (8)$$

where r = reflection coefficient = 0.1, in our case. B_3 is obtained as the difference between g [the larger root in (8)] and the real part of Y .

- b) For a given pair of B_1 and B_2 , we find the minimum value of B_3 , $B_{3,\min}$ (or surface resistivity $R_{3,\max}$), in the frequency range of f_0 to f_H .
- c) For each set B_1 , B_2 , and $B_{3,\min}$, we compute f_2 .

f_2 is found to be 1.60 f_0 and, therefore, $w = 1.20$, which agrees very well with [7]. It is found that the smallest and largest possible values of R_1 are 246 and $330 \Omega/\square$, respectively. Fig. 7 shows optimized pair of R_2 and $R_{3,\max}$ when R_1 equals $330 \Omega/\square$. It is noted that the optimized set of R_1 , R_2 , and $R_{3,\max}$ give three nulls in the reflection coefficient curve of the three-layer resistive sheet.

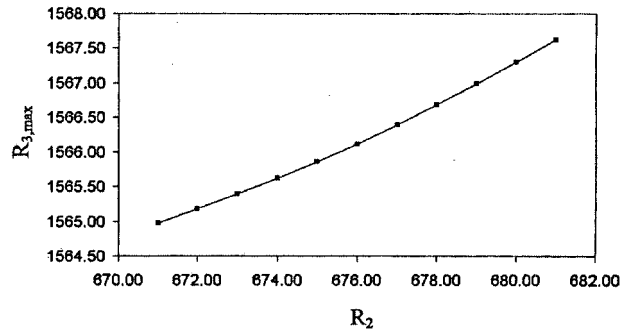


Fig. 7. Optimized R_2 and $R_{3,\max}$ when $R_1 = 330 \Omega/\square$ to obtain bandwidth of 0.86.

IV. CONCLUSION

The electrical engineer or material scientist can use the Smith Chart Approach to visualize how the design of the multilayer resistive sheet works. It also can be used to see whether the desired bandwidth is achievable in practice. Three examples on designing the multilayer resistive sheet by using the Smith Chart Approach were given. With the visualization using the Smith Chart, this approach offers more flexibility to the design of the multilayer resistive sheet, as compared to published formulae or tables.

REFERENCES

- [1] G. T. Ruck, D. E. Barrick, W. D. Stuart, and C. D. Krichgaum, *Radar Cross-Section Handbook*. New York: Plenum, 1970, pp. 612–617.
- [2] R. L. Fante and M. T. McCormack, “Reflection properties of the Salisbury screen,” *IEEE Trans. Antennas Propagat.*, vol. 36, pp. 1443–1454, 1988.
- [3] B. Chambers, “Optimum design of a Salisbury screen radar absorber,” *Electron. Lett.*, vol. 30, no. 16, pp. 1353–1354, 1994.
- [4] J. R. Nortier, C. A. Van der Neut, and D. E. Baker, “Tables for the design of Jaumann microwave absorbers,” *Microwave J.*, pp. 219–222, Sept. 1987.
- [5] L. J. Du Toit and J. H. Cloete, “A design process for Jaumann absorbers,” in *Antenna Propagat. Soc. Int. Symp., AP-S Digest*, 1989, pp. 1558–1561.
- [6] B. Chambers and A. Tenant, “The optimized design of wide-band Jaumann radar absorbing materials using a genetic algorithm,” *Electron. Lett.*, vol. 30, no. 16, pp. 1626–1628, 1994.
- [7] L. J. Du Toit and J. H. Cloete, “Electric screen Jauman absorber design algorithms,” *IEEE Trans. Microwave Theory Tech.*, vol. 44, pp. 2238–2245, Dec. 1996.